TIGHT FOCUSING OF LASER LIGHT USING A SURFACE PLASMON POLARITON IN A SILVER NANO-STRIP AND NANO-RING ON SILICA GLASS

E.S. Kozlova [1,2], V.V. Kotlyar [1,2]

[1] *Image Processing Systems Institute of the RAS – Branch of the FSRC "Crystallography and Photonics" RAS, Samara, Russia,*
[2] *Samara National Research University, Samara, Russia*

Abstract

In this work a solitary surface plasmon-polariton was obtained by using a frequency-dependent finite difference time-domain method for the TM- and radially polarized light at 532 nm, which was propagated through silver nano-elements (a nano-strip and a nano-ring), placed in an aqueous medium. The device's height and width were equal to 20 nm and 215 nm respectively. The intensity of surface plasmon-polariton was four times higher than that of the incident radiation. The full width at half maximum of the nanojet was 138 nm and 158 nm for the case of using a nano-strip and a nano-ring respectively. The results can be used to design devices that allow capturing and moving particles in water or other biofluids.

Introduction

Today great attention is paid to such optical phenomena as surface plasmon-polaritons (SPPs) which arise during interaction of light with the metal and propagate along the interfaces between metal and dielectric [1 – 3]. SPP can be widely used to solve various problems of modern science and technology [4 – 8]. The plasmonic field represents an exciting new area for the application of SPPs in which surface-plasmon based circuits merge the fields of photonics and electronics at the nanoscale [9]. The SPPs can serve as a basis for constructing nanoscale photonic circuits that will be able to carry optical signals and electric currents [10, 11]. SPPs can also serve as a basis for the design, fabrication and characterization of subwavelength waveguide components [12 – 15]. In the framework of plasmonics, modulators and switches have also been investigated [16, 17], as well as the use of SPPs as mediators in the transfer of energy from donor to acceptors molecules on opposite sides of metal films [18]. Application of SPPs enables subwavelength optics in microscopy and lithography beyond the diffraction limit [19, 20]. It also enables the first steady-state micromechanical measurement of a fundamental property of light itself: the momentum of a photon in a dielectric medium. Other applications are photonic data storage [21] and light generation [22].

A large number of works devoted to the modeling of nano-antennas, based on SPP's excitation effect [23, 24]. A Fabry-Perot model was formulated that predicts both the peak position and spectral shape of optical resonances for short-range SPP. The authors used full-field simulation based on the finite-difference time-domain method (FDTD-method) to calculate the parameters for this model [23]. Whereas, some other authors used rectangular gold and silver nano-strips embedded in glass or water. The effect of SPP's resonance is analyzed using a surface integral equation method. They showed the feasibility of at least 10-fold field magnitude enhancement for local field in narrow (5 nm) gap between two metal strips [24]. But all these authors didn't investigate another properties of SPP like length and full width at half maximum (FWHM).

In our previous work we have investigated the amplitude Fresnel zone plate for focusing of laser light. During this study we have found SPP's on surface of silver relief of this zone plate [25]. In this paper, we used the frequency-dependent FDTD-method ((FD)²TD-method) for investigating the process of SPP's formation on silver nano-strip for the incident TM-polarized light at 532 nm. We estimated spatial characteristics such as length and FWHM of SPPs which is new investigation up to our knowledge. We also used the (FD)²TD-method for investigating the process of SPP's formation on silver nano-ring for the incident radial-polarized light at 532 nm. The estimation of spatial characteristics such as length and FWHM of SPPs also was carried out. In contrast to the works described above, silver elements (nano-strip and nano-ring) are placed on a silica glass, which has a high influence on the process of SPP's formation.

Formation of SPPs on silver nano-strip

We considered the propagation of a TM-polarized light at 532 nm, which was normally incident on the metal nano-strip placed on a substrate. The optical scheme is presented on Fig. 1. Height and width of nano-strip are h and w respectively. The permittivity of the medium, nano-strip and substrate are ε_1, ε_m and ε_2 respectively. The light is propagating along Z axis. All the simulations were carried out by Full-WAVE (RSoft) based on (FD)²TD-method. Hereinafter, the following simulation parameters were used: spatial steps

were 2 nm, time step was 1 nm (ct, where c is speed of light in vacuum, t is a time).
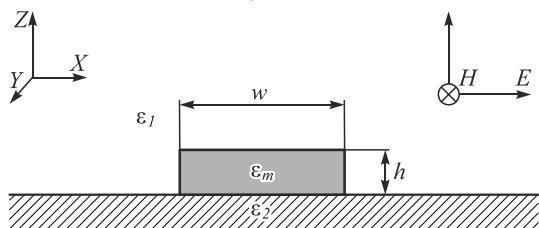

Fig. 1. Optical scheme for nano-strip

Silica glass was considered as a material of substrate. Table 1 shows parameters for the Sellmeier's permittivity model of silica glass [26]:

$$\varepsilon_2(\lambda) = \varepsilon_\infty + \sum_m \frac{\Delta\varepsilon_m \lambda^2}{\lambda^2 - \lambda_m^2 - i\lambda\eta_m}, \quad (1)$$

where λ is a wavelength; $\varepsilon_\infty(x, z)$ is the permittivity in the limit of infinite frequency; $\Delta\varepsilon_m$ is the resonance strength; λ_m is the resonant wavelength; η_m is the Sellmeier damping factor.

Table 1. Parameters for the Sellmeier's permittivity model of silica glass

m	$\Delta\varepsilon_m$	λ_m, μm	η_m, μm
1	0.69616630	0.068404300	0
2	0.40794260	0.11624140	0
3	0.89747940	9.8961610	0
$\varepsilon_\infty = 1$			

Silver was considered as a material of nano-strip. Table 2 shows parameters for the Drude-Lorentz's permittivity model of silver [27]:

$$\varepsilon_m(\omega) = \varepsilon_\infty + (\omega_p^2 / (-2i\omega\nu - \omega^2)) +$$
$$+ \sum_m (A_m\omega_m^2 / (-\omega^2 - 2i\omega\delta_m + \omega_m^2)), \quad (2)$$

where ω is a frequency; ω_p is the plasma frequency; ν is the collision frequency; A_m is the resonance strength; δ_m is the damping factor; ω_m is the resonant frequency.

Table 2. Parameters for the Drude-Lorentz's permittivity model of silver

m	A_m	δ_m, Hz	ω_m, Hz
1	7.924697	19.68071	4.132646
2	0.501327	2.289161	22.6941
3	0.013329	0.329194	41.45307
4	0.826552	4.639097	46.001
5	1.113336	12.25	102.759
$\varepsilon_\infty = 1$			
$\omega_p = 41.94605$ Hz			
$\nu = 0.243097$ Hz			

For the first series of simulation we fixed the strip height equals to $h = 20$ nm, remove the substrate and choose air ($\varepsilon_{1} = 1$) as a medium. After each calculation, we measured the maximum intensity of light at 2 nm above the nano-strip. Fig. 2 shows the SPP's intensity dependence on nano-strip width. These results are consistent with the results of other authors in similar calculations which have been carried out for nano-strips with other dimensions (thickness and width) [23, 24].
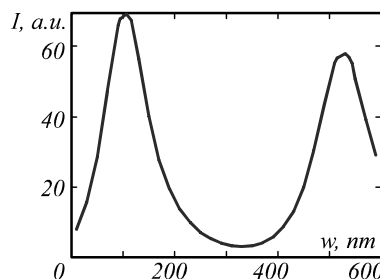

Fig. 2. The SPP's intensity dependence on nano-stip width for incident light at 532 nm

By comparing the simulation results for light propagation through the silver nano-strip of various widths, the resonant width $w = 110$ nm has been selected. Nano-strip with this width forms a "boundary" SPPs with the highest value of the intensity in the central peak. Fig. 3 shows the intensity distribution obtained at 2 nm above silver nano-strip with width of $w = 110$ nm.
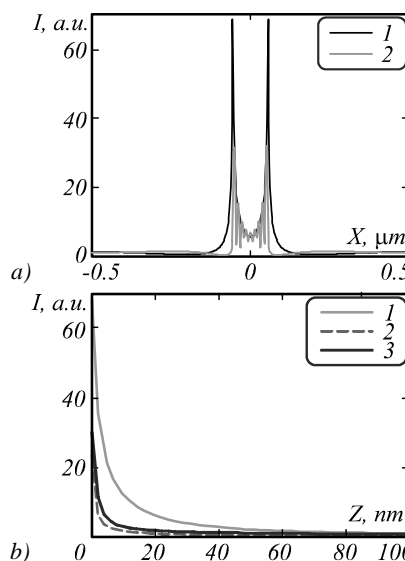

Fig. 3. (a) Intensity distribution at 2 nm above silver nano-strip of width, $w = 110$ nm placed in air (line 1) and on the silica glass placed in water (line 2). (b) SPP's intensity distribution through the direction of light propagation in the case of using nano-strip placed in air (line 1) and nano-strip on the silica glass placed in air (line 2) and water (line 3)

Two powerful "boundary" SPP (line 1) with high intensity (68 a.u.) and small FWHM (8 nm) can be seen from Fig. 3a. Fig. 3b shows the intensity distribution in the SPP along axis of light propagation. Measurement of SPPs "length" showed that the distance of decline to incident intensity through the Z direction is 68 nm, while through the direction of SPPs propagation it is 94 nm (Fig. 3b, line 1). The inclination angles of straight which were coinciding with the directions of SPPs propagation are 112° and 68°.

For the next simulations the substrate from silica glass was added. In this case, the direction of SPPs propagation changed and practically coincided with the direction of light propagation (it was parallel to the Z axis). However, the presence of the substrate substantially disrupts the formation of the SPP. It leads to fluctuations at the interface substrate/strip environments, reduces the maximum

intensity and "length" till 20 nm (Fig. 3*b*, line 2) of "boundary" SPPs.

To compensate this effect, water ($\varepsilon_1 = 1.78$) was chosen as a main medium instead of air. In this case measurement of SPPs "length" showed that the distance of decline to incident intensity through the *Z* direction is 56 nm (Fig. 3*b*, line 3). FWHM of "boundary" SPPs is 75 nm (Fig. 3*a*, line 2). The intensity of "boundary" SPPs is 36 times higher than intensity of incident light (Fig. 3*a*, line 2). However, the use of such sharply focused light is complicated by the close proximity of these peaks to each other and the presence of the boundary plasmonic lobes, which are formed along the entire nano-strip.

In addition to "boundary" short-range SPPs which have a maximum intensity, there are other SPPs. However, during the study of dependences of SPP's intensity distribution on the width of nano-strip placed in the air shows no possibility to obtain a "long" single SPP in the center of nano-strip. A similar study for the nano-strip placed on the silica glass in an aqueous medium revealed the presence of this "central" SPP. By comparing the simulation results for light propagation through the silver nano-strip of various widths, the width $w = 215$ nm has been selected. Fig. 4 shows the intensity distribution at 6 nm above silver nano-strip with width of $w = 215$ nm.
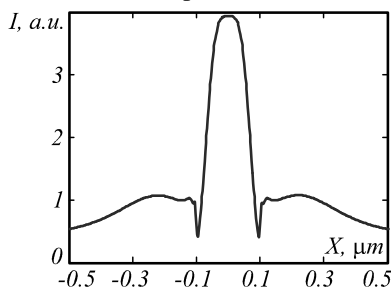

Fig. 4. Intensity distribution 6 nm after silver nano-strip with width of w = 215 nm o silica glass in water

Fig. 4 shows that the "boundary" SPPs is almost completely absent. FWHM of "central" SPP is 138 nm. The intensity of "central" SPP is four times higher than intensity of incident light (Fig. 4). The measurement of SPP "length" showed that the decay length to incident intensity through *Z* direction is 54 nm. The "central" SPP is also observed on the silver nano-strip with width of $w = 215$ nm placed on silica glass in air, but "boundary" SPPs are also present and their intensity is comparable with the intensity of "central" SPP.

Formation of SPPs between silver nano-srips

In this part we considered the propagation of a TM-polarized light at 532 nm, which was normally incident on the gap between two metal nano-strips placed on a substrate. The optical scheme is presented on Fig. 5. Height and width of nano-strips are *h* and *w* respectively. The width of the gap is w_h. The light is propagating along *Z* axis.

The height of nano-srtips was fixed at 10 nm as in [24]. By comparing the simulation results for light propagation through the gap between two silver nano-strip of various widths, the resonant widths of strips $w = 55$ nm and gap $w_h = 6$ nm have been selected. Gap with this

width forms a SPPs with the highest value of the intensity in the central peak. Simulations were carried out for both cases in air and in water. Fig. 6 shows the intensity distribution obtained at 2 nm above silver nano-strips.
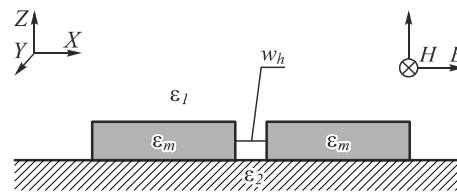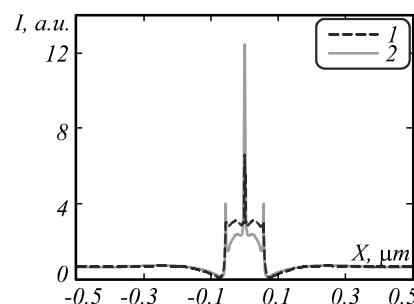

Fig. 5. Optical scheme for two nano-strips

Fig. 6. Intensity distribution at 2 nm above silver nano-strips of width w = 55 nm with gap of 6 nm between them. Strips are on the silica glass placed in air (line 1) or in water (line 2)

Powerful "boundary" SPPs with high intensity (6.2 a.u. in air and 13.3 a.u. in water) and small FWHM (2 – 3 nm) can be seen from Fig. 6. Unfortunately, measurement of SPPs "length" showed that the distance of decline to incident intensity through the *Z* direction is near 10 nm. This radiation is "gripped in a vice" of metal strips.

Formation of SPPs on silver nano-ring

In previous part we show the presence of "central" SPP on silver nano-strip with width of 215 nm in aqueous medium. In this part we considered the formation of "central" SPPs on silver nano-ring placed on a substrate. We considered the propagation of light at 532 nm, which was normally incident on the metal nano-ring. The radial polarization is selected to satisfy the condition of formation of SPPs. The optical scheme is presented on Fig. 7. Height of nano-ring is *h*. Width and internal radius (the distance from the centre of symmetry to the center line of the circle) of nano-ring are w_c and *R* respectively. The permittivity of the medium, nano-ring and substrate are ε_1, ε_m and ε_2 respectively. The light is propagating along *Z* axis. All the simulations were carried out by FullWAVE. Hereinafter, the following simulation parameters were used: steps in space were $\lambda / 30$ nm, time step was $\lambda / 60$ nm (*ct*).
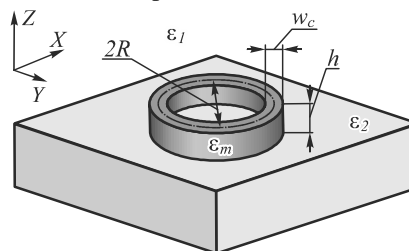

Fig. 7. Optical scheme for nano-ring: light propagates from the bottom up

The incident field was calculated in MATLAB and was set from file into FullWAVE to produce radial polarization. The calculation was carried out by using next equations for each component of the field:

$$
\begin{cases}
E_x = \dfrac{2\sqrt{2} \cdot x}{\delta} e^{-\frac{x^2+y^2}{\delta^2}}; \\[3mm]
E_y = \dfrac{2\sqrt{2} \cdot y}{\delta} e^{-\frac{x^2+y^2}{\delta^2}},
\end{cases}
\tag{3}
$$

where E_x and E_y are the components of electric field, δ is the waist of Gaussian beam.

The radius of waist of both Gaussian beams (for E_x and E_y components) was chosen equal to 0.5 µm and maximum intensity was normed to 1 a.u. Fig. 6 shows the incident light for simulation.

It can be seen from the Fig. 8 that the maximum of input intensity is at the radius of 0.5 µm, so the internal radius $R = 0.5$ µm is chosen to ensure that the maximum intensity of the radiation fell on the circle.
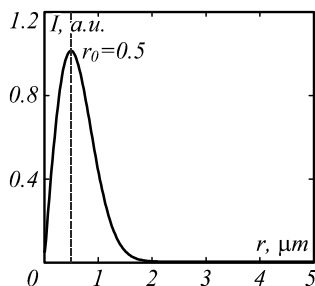

Fig. 8. Input radial polarized light with waist $\delta = 0.5$ µm: distribution along the radius r

A similar to previous study for the nano-ring placed on the silica glass in an aqueous medium revealed the presence of this "central" SPP. By comparing the simulation results for light propagation through the silver nano-ring of various widths, the width $w = 215$ nm has also been selected. Fig. 9 shows the intensity distribution at $\lambda/15$ nm above silver nano-ring with width of $w = 215$ nm.

Fig. 9a shows that the "central" SPP is evenly located on the whole surface of the circle. Fig. 9b shows that the "boundary" SPPs is almost completely absent. FWHM of "central" SPP is 158 nm. The intensity of "central" SPPs at $\lambda/15$ nm above silver nano-ring is three times higher than intensity of incident light (Fig. 9).

The measurement of SPPs "length" was also carried out. Fig. 10 shows the longitudinal distribution of light (distribution along the Z axis). It shows that the "length" of SPP through Z direction is 100 nm.

Conclusion

In this work the process of SPPs formation on silver nano-strip for TM-polarized light at 532 nm is studied. The spatial characteristics of SPPs like "length" and FWHM were investigated by using (FD)²TD-method. In contrast to the [23, 24], where silver nano-strips were considered to be placed into any media (water or silica glass), we consider them to be placed on a silica glass in air or water. In this case we can use the energy of SPPs for different application as optical tweezers or microscopy while using of scheme from [23, 24] we get this

energy in any substrate. Unfortunately the presence of several dielectrics with different values of permittivity in scheme brings a disturbance in the process of SPP's formation. It leads to fluctuations of field of light intensity at the interface substrate/strip environments, reduces the maximum intensity and "length" of SPP's. To compensate this effect, the water ($\varepsilon_1 = 1.78$) was chosen as a main medium instead of air. In this case measurement of SPPs "length" showed that the "length" of SPP through the Z direction is 56 nm (Fig. 3b, line 3). FWHM of "boundary" SPPs is 75 nm (Fig. 3a, line 2). The intensity of "boundary" SPPs is 36 times higher than intensity of incident light (Fig. 3a, line 2).

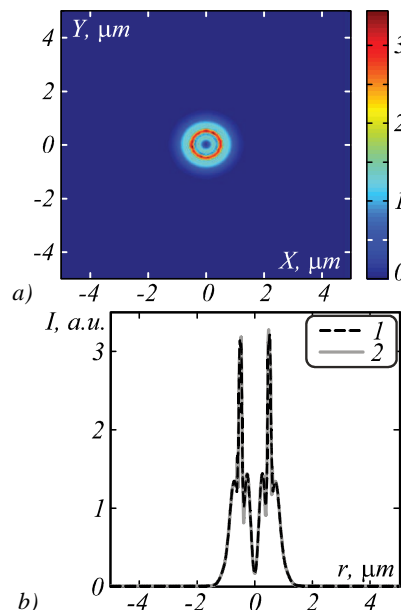*Fig. 9. Intensity distribution $\lambda/15$ nm after silver nano-ring with width of $w = 215$ nm on the silica glass placed in water: distribution at XY-plane (a) and along the radius r for $y = 0.5$ (line 1) and $x = 0.5$ (line 2)*
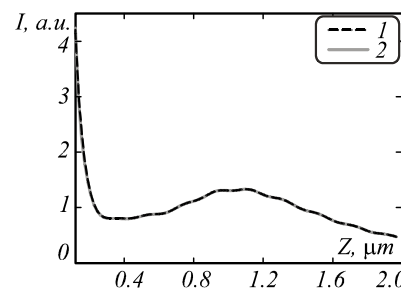

Fig. 10. SPP's intensity distribution through the direction of SPP's propagation in the case of using nano-ring placed on the silica glass in water fixing (x,y) at (0, 0.5) (line 1) and at (0.5,0) (line 2)

Analogous investigation for narrow gap between two nano-strips was carried out. Powerful "boundary" SPPs with high intensity (13.3 a.u. in water) and small FWHM ($2-3$ nm) was obtained. The intensity of this SPPs is in 1.1 times bigger than the intensity of SPPs in [24] while the nano-strips were considered to be placed on silica glass.

Simulations by (FD)²TD-method showed presence of "central" SPP for silver nano-strip placed in water. FWHM of "central" SPP is 138 nm. The intensity of "central" SPPs is four times higher than the intensity of incident light (Fig. 4). The "boundary" SPPs is almost completely ab-

sent. This result was generalized for 3D case for radial polarized light and nano-ring. Simulations by (FD)²TD-method showed presence of "central" SPP for silver nanoring placed on silica glass in water. FWHM of "central" SPP is 158 nm. The intensity of "central" SPPs is four times higher than the intensity of incident light (Fig. 10). The "boundary" SPPs are also almost completely absent. Unlike plasmonic lens with Archimedes spiral slot etched on it [28, 29], a nano-strips and nano-ring are easy to manufacture and also focuses light in a narrower area: the FWHM is 0.26λ (FWHM is 0.35λ in [28, 29]).

Investigation of convergence of solutions was also carried out. Reducing of the dimensions of the grid twice did not lead to significant changes in the results of the simulation. In particular, the FWHM of the focal spot is not changed, and the maximum intensity is slightly decreased.

The results can be used to design devices that allow capturing and moving the particles in water or other biofluidics [30, 31].

References

[1] Bezus EA, Doskolovich LL. Phase modulation and refraction of surface plasmon polaritons with parasitic scattering suppression. Computer Optics 2014; 38(4): 623-628. DOI: 10.18287/0134-2452-2014-38-4-623-628.

[2] Bezus EA, Doskolovich LL, Kazanskiy NL. Low-scattering surface plasmon refraction with isotropic materials. Opt Express 2014; 22(11): 13547-13554. DOI: 10.1364/OE.22.013547.

[3] Soifer, VA, Kotlyar VV, Doskolovich LL. Diffractive optical elements in nanofotonics devices [In Russian]. Computer Optics 2009; 33: 352-368.

[4] Kadomina EA, Bezus EA, Doskolovich LL. Resonant photonic-crystal structures with a diffraction grating for refractive index sensing [In Russian]. Computer Optics 2016; 40: 164-172. DOI: 10.18287/2412-6179-2016-40-2-164-172.

[5] Ma R-M, Oulton RF, Sorger VJ, Zhang X. Plasmon lasers: coherent light source at molecular scales. Laser & Photonics Reviews 2013; 7(1): 1-21. DOI: 10.1002/lpor.201100040.

[6] Xie Zh, Yu W, Wang T, Zhang H, Fu Yo, Liu H, Li F, Lu Zh, Sun Q. Plasmonic Nanolithography: A Review. Plasmonics 2011; 6: 565-580. DOI: 10.1007/s11468-011-9237-0.

[7] Han Z, Bozhevolnyi SI. Radiation guiding with surface plasmon polaritons. Reports on Progress in Physics 2013; 76(1): 016402. DOI: 10.1088/0034-4885/76/1/016402.

[8] Atwater HA, Polman A. Plasmonics for improved photovoltaic devices. Nature Materials 2010; 9: 205-213. DOI: 10.1038/nmat2629.

[9] Ozbay E. Plasmonics merging photonics and electronics at nanoscale dimentions. Science 2006; 311(5758): 189-193. DOI: 10.1126/science.1114849.

[10] Barnes WL, Dereux A, Ebbesen TW. Surface plasmon subwavelength optics. Nature 2003; 424: 824-830. DOI: 10.1038/nature01937.

[11] Nomura W, Ohtsu M, Yatsui T. Nanodot coupler with a surface plasmon polariton condenser for optical far/near-field conversion. Appl Phys Lett 2005; 86(18): 181108. DOI: 10.1063/1.1920419.

[12] Maier SA, Friedman MD, Barclay PE, Painter O. Experimental demonstration of fiber-accessible metal nanoparticle plasmon waveguides for planar energy guiding and sensing. Appl Phys Lett 2005; 86(7): 071103. DOI: 10.1063/1.1862340.

[13] Berini P, Charbonneau R, Lahoud N, Mattiussi G. Characterization of long-range surface-plasmon-polariton wave-guides. J Appl Phys 2005; 98(4): 043109. DOI: 10.1063/1.2008385.

[14] Bozhevilnyi SI, Volkov VS, Devaux E, Ebbesen TW. Channel Plasmon-Polariton Guiding by Subwavelength Metal Grooves. Phys Rev Lett 2005; 95: 046802. DOI: 10.1103/PhysRevLett.95.046802.

[15] Bozhevilnyi SI, Volkov VS, Devaux E, Laluet JY, Ebbesen TW. Channel plasmon subwavelength waveguide components including interferometers and ring resonators. Nature 2006; 440: 508-511. DOI: 10.1038/nature04594.

[16] Krasavin AV, Zheludev NI. Active plasmonics: Controlling signals in Au/Ga waveguide using nanoscale structural transformations. Appl Phys Lett 2004; 84(8): 1416-1418. DOI: 10.1063/1.1650904.

[17] Krasavin AV, Zayats AV, Zheludev NI. Active control of surface plasmon–polariton waves. J Opt A: Pure Appl Opt 2005; 7(2): S85. DOI: 10.1088/1464-4258/7/2/011.

[18] Andrew P, Barnes WL. Energy transfer across a metal film mediated by surface plasmon polaritons. Science 2004; 306(5698): 1002-1005. DOI: 10.1126/science.1102992.

[19] Kim ES, Kim YM, Choi KC. Surface plasmon-assisted nano-lithography with a perfect contact aluminum mask of a hexagonal dot array. Plasmonics 2016; 11(5): 1337-1342. DOI: 10.1007/s11468-016-0180-y.

[20] Luo X, Ishihara T. Surface plasmon resonant interference nanolithography technique. Appl Phys Lett 2004; 84(23): 4780-4782. DOI: 10.1063/1.1760221.

[21] Ditlbacher H, Krenn JR, Lamprecht B, Leitner A, Aussenegg FR. Spectrally coded optical data storage by metal nanoparticles. Opt Lett 2000; 25(8): 563-565. DOI: 10.1364/OL.25.000563.

[22] Kim S, Jin J, Kim Yo-J, Park I-Yo, Kim Yu, Kim S-W. High-harmonic generation by resonant plasmon field enhancement. Nature 2008; 453(7196): 757-760. DOI: 10.1038/nature07012.

[23] Søndergaard T. and Bozhevolnyi SI. Metal nano-strip optical resonators. Opt Express 2008; 15(7): 4198-4204. DOI: 10.1364/OE.15.004198.

[24] Barnard ES, White JS, Chandran A, Brongersma ML. Spectral properties of plasmonic resonator antennas. Opt Express 2008; 16(21): 16529-16537. DOI: 10.1364/OE.16.016529.

[25] Kozlova ES, Kotlyar VV, Nalimov AG. Comparative modeling of amplitude and phase zone plates [In Russian]. Computer Optics 2015; 39: 687-693. DOI: 10.18287/0134-2452-2015-39-5-687-693.

[26] Couairon A, Sudrie L, Franco M, Prade B, Mysyrowicz A. Filamentation and damage in fused silica induced by tightly focused femtosecond laser pulses. Phys Rev B 2005; 71(12): 125435-125441. DOI: 10.1103/PhysRevB.71.125435.

[27] Vial A, Laroche T, Dridi M, Le Cunff L. A new model of dispersion for metals leading to a more accurate modeling of plasmonic structures using the FDTD method. Appl Phys A 2011; 103(3): 849-853. DOI: 10.1007/s00339-010-6224-9.

[28] Huang F, Jiang X, Yuan H, Li S, Yang H, Sun X. Centrally Symmetric Focusing of Surface Plasmon Polaritons with a Rectangular Holes Arrayed Plasmonic Lens. Plasmonics 2016; 1-7. DOI: 10.1007/s11468-016-0220-7.

[29] Liu J, Gao Y, Ran L, Guo K, Lu Z, Liu S. Focusing surface plasmon and constructing central symmetry of focal field with linearly polarized light. Appl Phys Lett 2015; 106: 013116. DOI: 10.1063/1.4905307.

[30] Porfirev AP, Kovalev AA, Kotlyar VV. Optical trapping and moving of microparticles using asymmetrical bessel-gaussian beams [In Russian]. Computer Optics 2016; 40(2): 152-157. DOI: 10.18287/2412-6179-2016-40-2-152-157.

[31] Porfirev AP, Skidanov RV. Optical capture of microparticles in special traps [In Russian]. Computer Optics 2012; 36(2): 211-218.

Authors' information

Elena Sergeevna Kozlova, (b. 1989) received Master's degree in Applied Mathematics and Informatics from Samara State Aerospace University (2011). She received her Candidate's degree in Physics and Math in 2014. She is a researcher at the Laser Measurements laboratory at the Image Processing Systems Institute – Branch of the Federal Scientific Research Centre "Crystallography and Photonics" of the Russian Academy of Sciences and an assistant of the Computer Science department at Samara National Research University. Current research interests include diffractive optics, FDTD-method, near-field optics. E-mail: *kozlova.elena.s@gmail.com* .

Victor Victorovich Kotlyar (b. 1957) is the head of a laboratory at IPSI RAS – Branch of the FSRC "Crystallography and Photonics" RAS and a professor of Computer Science department at Samara National Research University. He graduated from Kuibyshev State University (1979), received his Candidate's and Doctor's Degrees in Physics & Mathematics from Saratov State University (1988) and Moscow Central Design Institute of Unique Instrumentation of the RAS (1992). He is a co-author of 300 scientific papers, 5 books and 7 inventions. His current research interests include diffractive optics, gradient optics, nanophotonics, and optical vortices. E-mail: *kotlyar@smr.ru* .